PROCEEDINGS OF SCIENCE

QCD Resummation in Dijet Azimuthal Angular Correlations at the Collider

Feng Yuan*

Nuclear Science Division, Lawrence Berkeley National Laboratory, Berkeley, CA 94720, USA
E-mail: fyuan@lbl.gov

We review recent theoretical developments in QCD resummation in dijet azimuthal angular correlation in hadronic collisions. The relevant coefficients for the Sudakov resummation factor, the soft and hard factors, are calculated. The theory predictions agree well with the experimental data from Tevatron and the LHC.

XXIII International Workshop on Deep-Inelastic Scattering,
27 April - May 1 2015
Dallas, Texas

*This material is based upon work supported by the U.S. Department of Energy, Office of Science, Office of Nuclear Physics, under contract number DE-AC02-05CH11231.

PoS(DIS2015)159

1. Introduction

Dijet production in hadronic collisions is one of the most simple process to study perturbative QCD and hadron physics in high energy experiments,

$$A+B \to Jet_1 + Jet_2 + X \ , \tag{1.1}$$

where A and B represent the two incoming hadrons with momenta P and $\overline{P}$, respectively, the azimuthal angle between the two jets is defined as $\phi = \phi_1 - \phi_2$ with $\phi_{1,2}$ the azimuthal angles of the two jets. Experiments at the Tevatron and LHC have studied this process extensively [1, 2, 3]. Most of dijet events are produced in the back-to-back configuration in the transverse plane, i.e., $\phi \sim \pi$. In particular, the leading order contributes to a Delta function at $\phi = \pi$. Singular behavior will show up at higher order corrections [4]. This divergence arises when the total transverse momentum of dijet (imbalance) is much smaller than the individual jet momentum, $q_\perp = |\vec{P}_{1\perp} + \vec{P}_{2\perp}| \ll |P_{1\perp}| \sim |P_{2\perp}| \sim P_T$, where large logarithms appear in every order of perturbative calculations. These large logs are normally referred as the Sudakov logarithms, $\alpha_s^i \ln^{2i-1}(P_T^2/q_\perp^2)$. Therefore, a QCD resummation has to be included in order to have a reliable theoretical prediction, which is referred as the transverse momentum dependent (TMD) resummation or the Collins-Soper-Sterman (CSS) resummation [5]. In this talk, we will summarize recent theoretical developments in applying the CSS technique in dijet production processes [6, 7, 8, 9, 10]. At the next-to-leading logarithmic (NLL) order, the resummation formula can be summarized as [9, 10],

$$\frac{d^4\sigma}{dy_1 dy_2 dP_T^2 d^2q_\perp} = \sum_{ab} \sigma_0 \left[\int \frac{d^2\vec{b}_\perp}{(2\pi)^2} e^{-i\vec{q}_\perp\cdot\vec{b}_\perp} W_{ab\to cd}(x_1, x_2, b_\perp) + Y_{ab\to cd} \right] \ , \tag{1.2}$$

where y_1 and y_2 are rapidities of the two jets, P_T is the leading jet transverse momentum, and $q_\perp$ the imbalance transverse momentum between the two jets as defined above. All order resummation for W from each partonic channel $ab \to cd$ can be written as

$$\begin{aligned} W_{ab\to cd}(x_1, x_2, b) &= x_1 f_a(x_1, \mu = b_0/b_\perp) x_2 f_b(x_2, \mu = b_0/b_\perp) e^{-S_{\rm Sud}(Q^2, b_\perp)} \\ &\times \ \mathrm{Tr}\left[\mathbf{H}_{ab\to cd} \exp[-\int_{b_0/b_\perp}^{Q} \frac{d\mu}{\mu} \gamma^{s\dagger}] \mathbf{S}_{ab\to cd} \exp[-\int_{b_0/b_\perp}^{Q} \frac{d\mu}{\mu} \gamma^{s}] \right] \ , \end{aligned} \tag{1.3}$$

where $Q^2 = \hat{s} = x_1 x_2 S$, which represents the hard momentum scale, $b_0 = 2e^{-\gamma_E}$, $f_{a,b}(x, \mu)$ are parton distributions for the incoming partons a and b, $x_{1,2} = P_T \left(e^{\pm y_1} + e^{\pm y_2}\right)/\sqrt{S}$ are momentum fractions of the incoming hadrons carried by the partons. In the above equation, the hard and soft factors $\mathbf{H}$ and $\mathbf{S}$ are expressed as matrices in the color space of partonic channel $ab \to cd$, and γ^s are the associated anomalous dimensions for the soft factor. The Sudakov form factor S_{Sud} resums the leading double logarithms and the universal sub-leading logarithms,

$$S_{\rm Sud}(Q^2, b_\perp) = \int_{b_0^2/b_\perp^2}^{Q^2} \frac{d\mu^2}{\mu^2} \left[A \ln\left(\frac{Q^2}{\mu^2}\right) + B + D_1 \ln\frac{Q^2}{P_T^2 R_1^2} + D_2 \ln\frac{Q^2}{P_T^2 R_2^2} \right] \ , \tag{1.4}$$

where $R_{1,2}$ represent the cone sizes for the two jets. Here the parameters A, B, D_1, D_2 can be expanded perturbatively in α_s. At one-loop order, $A = C_A \frac{\alpha_s}{\pi}$, $B = -2C_A\beta_0 \frac{\alpha_s}{\pi}$ for gluon-gluon initial state, $A = C_F \frac{\alpha_s}{\pi}$, $B = \frac{-3C_F}{2} \frac{\alpha_s}{\pi}$ for quark-quark initial state, and $A = \frac{(C_F + C_A)}{2} \frac{\alpha_s}{\pi}$, $B = (\frac{-3C_F}{4} - C_A\beta_0) \frac{\alpha_s}{\pi}$ for gluon-quark initial state, D coefficient represents the final state jet contribution with $D = C_A \frac{\alpha_s}{2\pi}$ for gluon jet and $D = C_F \frac{\alpha_s}{2\pi}$ for quark jet.

PoS(DIS2015)159

2. Calculations at One-loop Order

It is illustrative to have a one-loop calculation to show the main feature of high order perturbative corrections, and demonstrate the associated factorization for this process. One-loop corrections come from four contributions: (a) virtual contributions; (b) soft gluon radiation (real); (c) jet contributions; (d) collinear gluon radiation associated with the incoming parton distributions. The virtual graphs have been studied in the literature [11]. The jet contributions are easy to derive following the examples of inclusive jet production, where we adopt the narrow jet approximation (NJA) [12, 13]. Collinear gluon radiation associated with incoming parton distributions also contribute to the finite imbalance transverse momentum. This part can be formulated according to the well-known DGLAP splitting. In Figs. 1 and 2, we show schematic diagrams for these contributions.

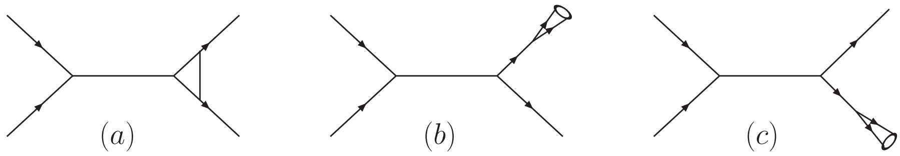

Figure 1: Schematic diagrams for virtual graph contribution (a) and final state jet contributions (b) and (c) at one-loop order. Both of them are proportional to a Delta function of the imbalance transverse momentum: $\delta^{(2)}(q_\perp)$.

As an example, let us show the result for the quark-quark scattering channel, $qq' \to qq'$, for which we have the following one-loop result for the dominant contributions in terms of large logarithms of $\ln(Q^2b_\perp^2/b_0^2)$ and $\ln(\mu^2b_\perp^2/b_0^2)$,

$$\begin{aligned} W^{(1)}(b_\perp)|_{logs.} \;&= \frac{\alpha_s}{2\pi}\left\{ h^{(0)}_{q_iq_j\to q_iq_j}\left[-\ln\left(\frac{\mu^2b_\perp^2}{b_0^2}\right)\left(\mathscr{P}_{qq}(\xi)\delta(1-\xi')+\mathscr{P}_{qq}(\xi')\delta(1-\xi)\right)-\delta(1-\xi)\right.\right.\\ &\times\delta(1-\xi')\left.\left(C_F\ln^2\left(\frac{Q^2b_\perp^2}{b_0^2}\right)+\ln\left(\frac{Q^2b_\perp^2}{b_0^2}\right)\left(-3C_F+C_F\ln\frac{1}{R_1^2}+C_F\ln\frac{1}{R_2^2}\right)\right)\right]\\ &\left.-\delta(1-\xi)\delta(1-\xi')\ln\left(\frac{Q^2b_\perp^2}{b_0^2}\right)\Gamma_{sn}^{(qq')}\right\}\,, \end{aligned} \tag{2.1}$$

where $h^{(0)}$ is the leading order expression for this partonic channel, $\mathscr{P}_{q/q}$ the quark-quark splitting kernel, and Γ_{sn} represents the process-dependent the sub-leading logarithmic term. A number of interesting features can be observed, which all support the associated QCD factorization and resummation. The large logarithms appear in the one-loop calculations contain three terms: (a) the

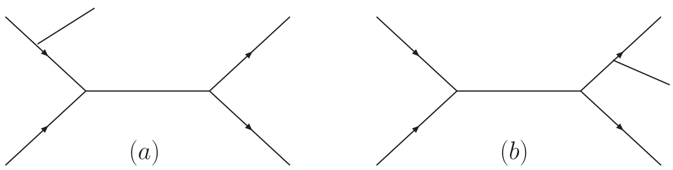

Figure 2: Schematic diagrams for real gluon radiation contribution to finite imbalance transverse momentum: (a) collinear gluon radiation associated with the incoming partons; (b) soft gluon radiation outside the jet cone of final state jets.

double logarithms in terms of $\ln^2(Q^2b_\perp^2/b_0^2)$ proportional to incoming partons color factors (here, it is $C_F + C_F$); (b) single logarithms in terms of $\ln(\mu^2 b_\perp^2/b_0^2)$ associated with parton distributions; (c) the left single logarithms of $\ln(Q^2b_\perp^2/b_0^2)$ contains similar terms as Drell-Yan process (the $-3C_F$ term) and those associated with dijet production in this particular channel (jet size dependent contributions and additional contributions which is process-dependent).

Another important cross check is to compare to the fixed order calculations in the correlation limit, i.e., $q_\perp \ll P_T$. To do that, we add the soft gluon (real) and collinear gluon (real) contributions together, which leads to the so-called asymptotic behavior for the differential cross sections at low imbalance transverse momentum $q_\perp$. This was compared to the fixed order calculations, and it was found that the asymptotic results agree well with the fixed order perturbative calculations in the correlation limit. This demonstrates that the most important contributions from the collinear and soft gluon radiation have been computed in the one-loop calculations [9, 10].

3. TMD Factorization and Resummation

To derive the QCD resummation formalism in dijet production process, we argue that a TMD factorization can be applied, where the differential cross section can be factorized into the TMD parton distributions, soft and hard factors. The final resummation was achieved by solving the relevant evolution equation for the TMDs and the soft factor. We adopt the Ji-Ma-Yuan scheme for the TMD parton distributions [14],

$$xg(x,k_\perp) = \int \frac{d\xi^- d^2\xi_\perp}{P^+(2\pi)^3} e^{-ixP^+\xi^- + i\vec{k}_\perp\cdot\vec{\xi}_\perp} \left\langle P|F_a^+{}_\mu(\xi^-,\xi_\perp)\mathcal{L}^\dagger_{vab}(\xi^-,\xi_\perp)\mathcal{L}_{vbc}(0,0_\perp)F_c^{\mu+}(0)|P\right\rangle ,$$

for the TMD gluon distribution, where $F^{\mu\nu}$ is the gauge field strength tensor, and

$$\mathcal{L}_v(\xi) = P\exp\left(-ig\int_0^{-\infty} d\lambda v\cdot A(\lambda v+\xi)\right)$$

is the gauge link in the adjoint representation, $A^\mu = -if_{abc}A_c^\mu$. The off-light-cone vector v is introduced to regulate the light-cone singularity associated with the TMD distributions, $\zeta^2 = (2v\cdot P)^2/v^2$. An evolution equation can be derived for the TMD distributions respect to ζ,

$$\frac{\partial}{\partial \ln\zeta} xg(x,b_\perp,\zeta) = (K(\mu,b_\perp)+G(\zeta,\mu))\times xg(x,b_\perp,\zeta) , \tag{3.1}$$

where K and G are the evolution kernel. Similarly, we will introduce the TMD parton distribution from incoming hadron B, which includes another light-cone singularity regulator $\bar{\zeta}^2 = (2\bar{v}\cdot\bar{P})^2/\bar{v}^2$. After resummation, the dependence on v and $\bar{v}$ will cancel out between TMD distributions and the soft factors.

In the dijet production process, there is an additional soft factor contribution in the TMD factorization, which depends on the color configuration of the partonic scattering channels. The first calculation to take into account the soft gluon contribution for dijet production was considered in Ref. [15, 16] in the context of the threshold resummation, where the soft gluon radiations are evaluated on the orthogonal color basis. We follow this procedure to formulate the soft factor in

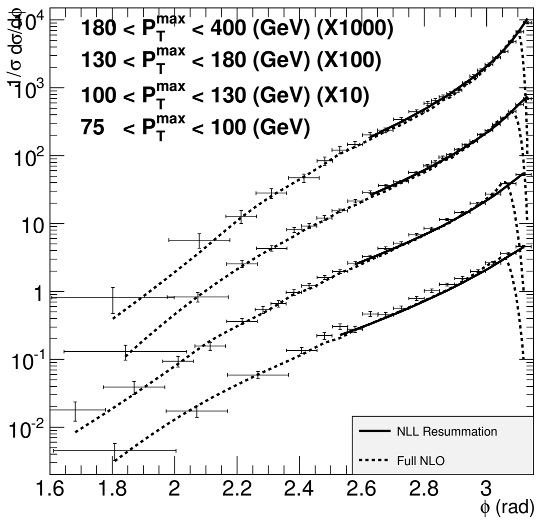

Figure 3: Resummation results on dijet azimuthal correlations at the Tevatron, compared to the experimental data from D0 Collaboration [1], where both jets are produced in central-rapidity region with $|y| < 0.5$. Away from $\phi = \pi$, the resummation results (solid curves) are matched to a full NLO calculation (dashed curves) [1, 4].

the same color bases for all partonic channels. After computing the one-loop diagrams of the soft factor, we find that the soft factor satisfies the renormalization group equation [15]:

$$\frac{d}{d\ln\mu} S_{IJ}(\mu) = -\Gamma^{s\dagger}_{IJ'} S_{J'J}(\mu) - S_{IJ'}(\mu)\Gamma^{s}_{J'J} \ , \tag{3.2}$$

where Γ is the relevant anomalous dimension. By solving the renormalization group equation, we resum the large logarithms associated with the soft factor.

Factorization implies that the differential cross section contributions from the partonic processes can be written as

$$W_{ab\to cd}(x_i,b) = x_1 f_a(x_1,b,\zeta^2,\mu^2,\rho) x_2 f_b(x_2,b,\bar{\zeta}^2,\mu^2,\rho) \mathrm{Tr}\left[\mathbf{H}_{ab\to cd}(Q^2,\mu^2,\rho)\mathbf{S}_{ab\to cd}(b,\mu^2,\rho)\right] \ ,$$

where the dependence on $\rho = (2v\cdot\bar{v})^2/v^2\bar{v}^2$ and the factorization scale μ cancel out among different factors. To derive the final resummation results, we have to solve the evolution equation for the parton distributions and the renormalization group equation for the soft factor. In particular, the factorization scale is chosen around $\mu = Q$, and evolve the parton distribution and soft factor from the scale $1/b$ to Q.

4. Compare to the Experimental Data

With resummation formula derived, we can compare to the experimental data. In Fig. 3, the Tevatron data from D0 Collaboration was shown. In the numeric calculations, the perturbative coefficients $A^{(1,2)}$, $B^{(1)}$ and $D^{(1)}_{1,2}$ are considered in the Sudakov form factor. When Fourier transforming the $b_\perp$-expression to obtain the transverse momentum distribution, we follow the b_* prescription

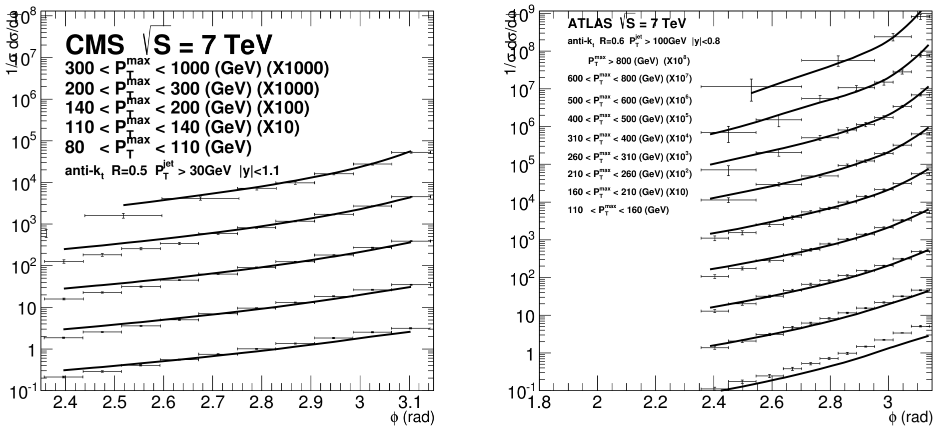

Figure 4: The comparisons between the resummation results and the experimental data from the CMS (left) and ATALAS collaborations at the LHC.

of CSS resummation [5], *i.e.*, replacing $b_\perp$ by $b_* = b/\sqrt{1+b^2/b_{max}^2}$ in the calculation. By doing so, we will also introduce the non-perturbative form factors for the quarks and gluons from the initial states. In our calculations, we have used $b_{max} = 0.5\,\text{GeV}^{-1}$, and the non-perturbative form factors follow the parameterizations in Refs. [17]. However, it was found that the final results are not sensitive to the non-perturbative form factors at all.

From Fig. 3, we see that the resummation results agree well with the experimental data, from ϕ near to π down to much smaller values. For smaller value of ϕ (away from the back-to-back configuration), the resummation calculations match to the fixed order results at NLO [4], which has also been separately shown in Fig. 3. We note that a full NLO calculation cannot describe experimental data for $\phi \sim \pi$ [1], where the fixed order calculation becomes divergent. Our resummation calculation, after being matched with the NLO result clearly improves the theory prediction and can describe the experimental data in a wider kinematic region.

In Fig. 4, we compare our resummation results with the experimental data from the LHC. Similar to the D0 measurements, the dijet measurements from CMS are presented in several kinematic bins, with the leading jet transverse momentum labelled by P_T^{max} in the figure. The second jet transverse momentum is chosen to be larger than 30 GeV. Both jets are in the mid-rapidity region, $|y_{jet}| < 1.1$. Anti-k_t jet algorithm with jet size $R = 0.5$ was used in the data analysis. In this figure, we limit the comparisons in the back-to-back correlation region, where we find perfect agreements between the resummation calculations and the experimental data over all transverse momentum bins. In ATLAS measurements [3], the same anti-k_t algorithm has been used, however, with jet size $R = 0.6$. The two jets are selected from the mid-rapidity region ($|y_{jet}| < 0.8$) with minimum transverse momentum of 100 GeV. Again, we find that the agreements between the resummation results and the experimental data are very well around the back-to-back correlation regions, except in the lowest P_T^{max} bin. The apparent poor agreement between the resummation prediction and the ATLAS data in the lowest P_T^{max} bin (between 110 GeV and 160 GeV) is caused by the stronger kinematic cut made on the second jet P_T, which is required to be above 100 GeV at ATLAS and 30 GeV at CMS. With a much tighter cut on this second jet P_T, the phase space for multiple soft gluon emission is limited so that our resummation calculation (which allows all possible soft gluon radiation) becomes less reliable in this case. We note that in the lowest P_T^{max} bin, the cross section is dominated by P_T^{max} around 110 GeV which is close to the 100 GeV cut on the second jet made by the ATLAS.

5. Conclusions

In this talk, we have summarized recent progress in QCD resummation calculation for dijet azimuthal angular correlation in hadron collisions. It was found that the perturbative expansion of the resummation calculation agree well with the fixed order calculation in the back-to-back correlation limit (ϕ around π). The resummation results can describe a much wider range of the experimental data, particulary for ϕ around π where event rate dominates. The agreements between the resummation results and the experimental data encourage further developments along this direction.

References

[1] V. M. Abazov *et al.* [D0 Collaboration], Phys. Rev. Lett. **94**, 221801 (2005).

[2] V. Khachatryan *et al.* [CMS Collaboration], Phys. Rev. Lett. **106**, 122003 (2011).

[3] G. Aad *et al.* [ATLAS Collaboration], Phys. Rev. Lett. **106**, 172002 (2011).

[4] Z. Nagy, Phys. Rev. Lett. **88**, 122003 (2002); Phys. Rev. D **68**, 094002 (2003).

[5] J. C. Collins, D. E. Soper and G. F. Sterman, Nucl. Phys. B **250**, 199 (1985).

[6] A. Banfi and M. Dasgupta, JHEP **0401**, 027 (2004).

[7] A. Banfi, M. Dasgupta and Y. Delenda, Phys. Lett. B **665**, 86 (2008).

[8] A. H. Mueller, B. -W. Xiao and F. Yuan, Phys. Rev. D **88**, 114010 (2013).

[9] P. Sun, C.-P. Yuan and F. Yuan, Phys. Rev. Lett. **113**, no. 23, 232001 (2014) [arXiv:1405.1105 [hep-ph]].

[10] P. Sun, C.-P. Yuan and F. Yuan, arXiv:1506.06170 [hep-ph].

[11] R. K. Ellis and J. C. Sexton, Nucl. Phys. B **269**, 445 (1986).

[12] B. Jager, M. Stratmann and W. Vogelsang, Phys. Rev. D **70**, 034010 (2004).

[13] A. Mukherjee and W. Vogelsang, Phys. Rev. D **86**, 094009 (2012).

[14] X. Ji, J. P. Ma and F. Yuan, Phys. Rev. D **71**, 034005 (2005); JHEP **0507**, 020 (2005).

[15] N. Kidonakis and G. F. Sterman, Nucl. Phys. B **505**, 321 (1997); N. Kidonakis, G. Oderda and G. F. Sterman, Nucl. Phys. B **525**, 299 (1998).

[16] J. Botts and G. F. Sterman, Nucl. Phys. B **325**, 62 (1989).

[17] F. Landry, R. Brock, P. M. Nadolsky and C. P. Yuan, Phys. Rev. D **67**, 073016 (2003); P. Sun, C. -P. Yuan and F. Yuan, Phys. Rev. D **88**, 054008 (2013); P. Sun, J. Isaacson, C.-P. Yuan and F. Yuan, arXiv:1406.3073 [hep-ph].

PoS(DIS2015)159